Title
Formation of exoplanetary satellites by pull-down capture

Journal
Science Advances, 5(10)

ISSN
2375-2548

Author
Hansen, Bradley MS

Publication Date
2019-10-04

DOI
10.1126/sciadv.aaw8665

Peer reviewed

ASTRONOMY

Formation of exoplanetary satellites by pull-down capture

Bradley M. S. Hansen

The large size and wide orbit of the recently announced exomoon candidate Kepler-1625b-i are hard to explain within traditional theories of satellite formation. We show that these properties can be reproduced if the satellite began as a circumstellar co-orbital body with the original core of the giant planet Kepler-1625b. This body was then drawn down into a circumplanetary orbit during the rapid accretion of the giant planet gaseous envelope, a process termed "pull-down capture." Our numerical integrations demonstrate the stability of the original configuration and the capture process. In this model, the exomoon Kepler-1625b-i is the protocore of a giant planet that never accreted a substantial gas envelope. Different initial conditions can give rise to capture into other co-orbital configurations, motivating the search for Trojan-like companions to this and other giant planets.

INTRODUCTION

The planetary satellites of the Solar system planets provide a wealth of information regarding the conditions under which the planets formed, reflecting the different pathways available in the inner and outer Solar system (*1*). Our attempts to understand the great variety of planetary types and architectures discovered around other stars would benefit greatly from similar information. Therefore, the recent announcement of a tentative detection of a bound companion to the transitting planet Kepler-1625b (*2*, *3*) is of potentially great importance. The precise properties of this observed system depend on the details of the analysis, but a representative value for the mass of the planet is $\sim 2M_J$, the mass of the satellite $\sim 10M_\oplus$, and the present distance of the exomoon from the planet $\sim 45R_J$. As shown in Fig. 1, this implies that the proposed satellite (hereafter called Kepler-1625b-i) has a mass and angular momentum far in excess of anything seen in the satellites of the Solar system planets. The parameters of Kepler-1625b-i are comparable to those of planets recently discovered orbiting close to low-mass stars. It is therefore not obvious that Kepler-1625b-i formed in a similar way to the Solar system moons.

The standard model for the formation of moons around gaseous planets is to form them from a disk of solid material in orbit. The origin of this disk has been variously hypothesized to be a solid-enhanced disk left behind by the initial collapse (*4*) or one that is fed by continuous accretion from the protoplanetary nebula (*5*). In either variant, the nominal mass of the resulting moons is well below the observed values for Kepler-1625b-i [e.g., (*6*)]. Population synthesis studies of these models can just reach the observed values (*7*), but in such cases, the amount of solid material added to the planet itself is such that the planet is enriched in solids-to-mass fractions ~50%. Such a large amount of solid enrichment would imply a planetary radius $\sim 0.8R_J$ (*8*), which is smaller than the observed radius (*2*). It appears as though that the Kepler-1625b-i system cannot be realized within the standard formalism developed for the Solar system giant planets.

Another suggested scenario is that the Kepler-1625b-i could be another planet that was captured by Kepler-1625b during a close encounter, in which tidal interactions dissipated enough energy to capture the planet. Such a process would capture the satellite into a highly eccentric orbit, which would eventually circularize to a much more compact configuration (*9*). There is, in principle, enough angular momentum in the spin of a newly formed giant planet (see Fig. 1) to drive the satellite outward (*10*), much as is believed to be the case in our own terrestrial system [e.g., (*11*)]. The problem here is one of time scale. Tidal interactions get rapidly weaker with distance, and the outward spiral of the orbit will be limited by the lifetime of the system. We can estimate the time scale to spiral out to the present orbit because of transfer of angular momentum from the planet to the satellite (*12*) as

$$T_p \sim 1.1 \times 10^{13}\,\mathrm{years}\left(\frac{M_s}{10M_\oplus}\right)^{-1}\left(\frac{a}{40R_J}\right)^{8}\frac{\sigma_J}{\sigma_p} \quad (1)$$

where M_s is the mass of Kepler-1625b-i and a is the semimajor axis of its planetocentric orbit. We have assumed a bulk tidal dissipation in the planet Kepler-1625b-i, σ_p, equivalent to that of Jupiter, σ_J, as calculated on the basis of the orbital evolution of the Jovian moons (*13*). This is orders of magnitude too long, given the age of the system. To quantify the discrepancy, we can also reverse the above argument to estimate the value necessary to achieve the desired level of outspiral. If we set $T_p = 10^{10}$ years, then we require $\sigma_p \sim 1100\,\sigma_J$. If we cast this in terms of the commonly quoted "tidal Q," then it would imply $Q \sim 25$ for the planet, a value more characteristic of a terrestrial planet than a gas giant. The conclusion that we draw from the above discussion is that all scenarios that assemble or capture Kepler-1625b-i after the host planet formed suffer from the problem that they produce moons that are either too small or too close.

We propose instead that Kepler-1625b-i became a satellite by the process of pull-down capture during the rapid accretion of the giant planet gaseous envelope (*14*). In the standard theory of giant planet formation by core accretion (*15*), the rocky cores of giant planets grow slowly by the accretion of planetesimals while maintaining a hydrostatically supported gaseous envelope. Eventually, the core grows large enough that gas pressure in the envelope can no longer support it against the planetary gravity and hydrostatic equilibrium in the envelope breakdown. At this point, the planet accretes gas on a dynamical time scale, until such time as it has opened a gap in the gaseous disk, which limits further supply. The final mass of the planet may grow further as gas is supplied to the planet by viscous transport through the disk (*16*), but a substantial fraction of the mass is accreted rapidly during this episode. The rapid growth in the planetary mass affects the dynamics of nearby bodies that share similar orbits to the

Mani Bhaumik Institute for Theoretical Physics, Department of Physics and Astronomy, UCLA, Los Angeles, CA 90095, USA. Email: hansen@astro.ucla.edu

growing planet. We will show that some fraction of these bodies can be drawn down into stable configurations that correspond to traditional satellite orbits.

MATERIALS AND METHODS

The original pull-down scenario (*14*) was used to describe the capture of low-mass irregular satellites to the giant planets of the solar system. Our first step was therefore to demonstrate that this process also operates when the initial co-orbital pair was of comparable mass. The numerical integrations used in this paper were performed by integrating the equations of motion for the direct gravitational interactions of three bodies using a Bulirsch-Stoer integrator. Although there are several programs in wide use for the integration of planetary system dynamics, they often use mass-dependent coordinate system transformations (such as Jacobi coordinates) to increase the efficiency and accuracy of the integration schemes. The use of these transformations can introduce subtle errors when the planetary masses are a function of time. Hence, we opted to numerically integrate a general three-body problem in a fixed coordinate system, only transferring to heliocentric coordinates at the end. In the Supplementary Materials, we demonstrate that the starting conditions for the pull-down scenario remain valid in this limit and that pull-down capture proceeds in a qualitatively similar fashion.

Figure 2 shows an example of such a pulldown. We started at one planet, the future giant planet, with a mass $m_2 = 30M_\oplus$, as expected from a giant planet core as it transitions from a hydrostatically supported envelope to runaway gas accretion (*15*). The other was assumed to have a mass $m_3 = 10M_\oplus$, as a representative value for Kepler-1625b-i. This can be viewed as a second protocore that lagged the former in growth rate and so has not yet reached the point of envelope instability. The pair was assumed to be in orbit about a 1-$M_\odot$ (solar mass) star with a semimajor axis of 1 astronomical unit. The initial positions and velocities were chosen such that the pair exhibits a quasi-periodic, retrograde orbit when viewed in the frame co-rotating with the larger of the pair. This planet was then assumed to grow according to

$$m_2 = 9 \times 10^{-5} + 2.11 \times 10^{-3}(1 - \exp(-T/100)) \qquad (2)$$

where the time scale is normalized such that the orbital period is 2π. The system was integrated for time $T = 500$. This describes a mass accretion rate that decays exponentially and was intended to describe

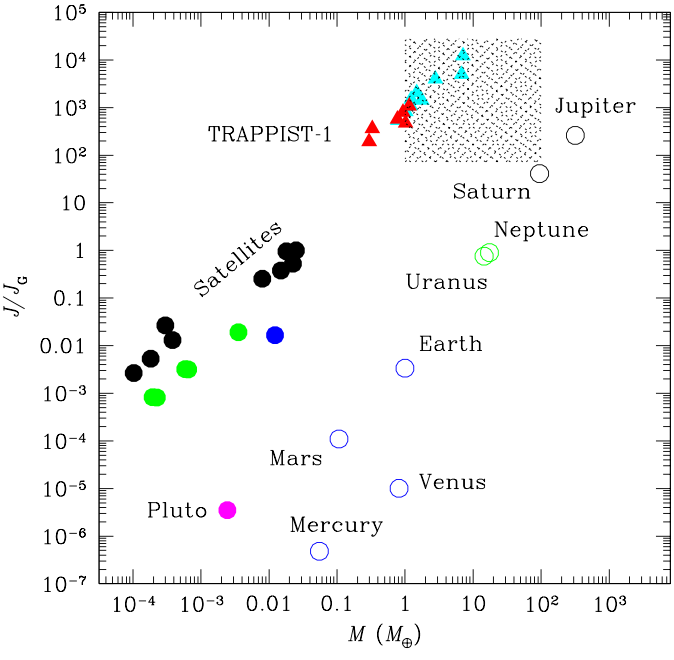

Fig. 1. Moon mass and angular momentum. The estimated mass, and orbital angular momentum, of the exomoon candidate Kepler-1625b-i is shown as the shaded region. This is compared to the masses and orbital angular momentum of the largest Solar system planetary satellites, shown as filled circles. The mass is normalized to the mass of the Earth, and the angular momentum J is normalized to J_G, the angular momentum of Ganymede about Jupiter. The masses of the Solar system planets are shown as open circles, plotted against the angular momentum contained in each planetary spin. Values associated with the terrestrial planets are plotted in blue; those associated with the gas giants Jupiter and Saturn are shown in black, and those associated with the ice giants Uranus and Neptune are shown in green. The Pluto-Charon binary dwarf planet is shown in magenta. The Solar system satellites fall short of Kepler-1625b-i by orders of magnitude. More comparable are the masses and orbital angular momenta of planets known to orbit very-low-mass stars. The system orbiting the low-mass star TRAPPIST-1 (*28*) are shown in red, while other planets known around stars with mass <0.2 $M_\odot$ (solar mass) are shown in cyan.

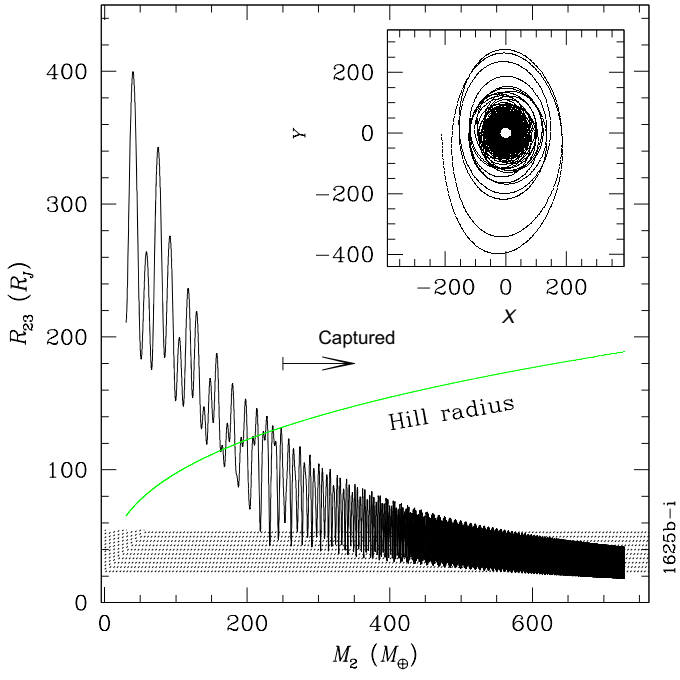

Fig. 2. The pulldown of an exomoon candidate due to the rapid growth of the giant planet. The black curve in the main plot shows the evolution of the separation R_{23} between the growing planet and its eventual satellite. The green curve shows the increase of the planetary Hill sphere as the mass grows, while the inset shows the evolution of the orbit itself in the original orbital plane, as seen in the frame co-moving with m_2. The shaded region shows the estimated location of the observed system. The elongation of the initial orbit is characteristic of the orbits classified as f-type in (*20*). As the moon is pulled down, the orbit becomes more circular, especially after it crosses the Hill sphere when the mass is ~0.75M_J, although it does retain a finite eccentricity and may be circularized by tides on a longer time scale.

the initially rapid accretion of mass that tails off as a gap is opened in the protoplanetary disk. The smaller body is dragged down by the changing gravitational potential to an orbit of final semimajor axis of $31R_J$, which lies within the estimated range for Kepler-1625b-i. Farther or closer orbits are easily obtained by starting with an initial binary of different separation.

To understand the dynamics, let us briefly return to the restricted problem ($m_3 = 0$) so that we may make use of a conserved integral, the Jacobi constant C. As the mass of m_2 grows, the orbit of m_2 about m_1 shrinks to conserve angular momentum. At any given moment in the evolution, the system can still be described in the context of the restricted three-body problem, but the value of C changes. The critical values of C that regulate the orbital dynamics also evolve with time but do not scale similarly with mass, as do the orbits. This means that the mass growth of m_2 can lead to a qualitative change in the orbit of a test particle if the value of C crosses a threshold value that separates one family of orbits from another.

To demonstrate this, we fixed our definition of the Jacobi constant to the original coordinate system so that the absolute value will evolve as the mass does, namely

$$C = 2\left(\frac{1}{R_{13}} + \frac{m_2}{R_{23}}\right) + \frac{1+m_2}{a^3}(x^2+y^2) - V^2 \qquad (3)$$

This has the same form as the traditional definition, but the numerical value will evolve as m_2. The quantities x, y (the components of the position of m_3 in the co-rotating orbital plane), and V (the velocity of m_3 in the co-rotating frame) are all defined relative to the center of mass and so will also evolve as the mass ratio changes. The semimajor axis a also evolves as the orbit shrinks. This was calculated directly from the equation for the orbital energy. The critical values of C, as a function of m_2, were calculated from the extrema of the instantaneous pseudopotential. Figure 3 shows the derivative $\partial C/\partial m_2$ for the case $m_2 = 9 \times 10^{-5}$ and $m_3 = 0$. We see that the derivative peaks near the planet (*17*), so that particles that spend a long time in the vicinity of the planet will be most affected by the mass growth. Figure 4 shows the evolution of three different initial orbits, indicated as filled circles in Fig. 3. The orbit shown in Fig. 4A experiences a substantial growth in C and soon crosses the critical values that define the L_2 and L_1 Lagrangian points. This is the formal criterion for pull-down capture, meaning that the planetary orbit is ultimately confined to the Hill sphere of m_2. The orbit shown in Fig. 4B demonstrates that the Lagrangian L_4 point is stable and that particles exhibiting this kind of tadpole orbit only become more tightly bound upon mass growth of m_2. In Fig. 4C, we see that horseshoe orbits that pass around the L_3 point can be also pulled down into tadpole orbits, in this case about the L_5 point.

RESULTS

An important potential discriminant between the pull-down capture model and traditional satellite formation models is that this model generically produces final satellite orbits that have substantial eccentricity and orbital inclination (defined here as the angle between the angular momentum vectors of the m_3 to m_2 orbit relative to the m_2 to m_1 orbit). Although there is no observational constraint on the orbital eccentricity of Kepler-1625b-i, there is weak evidence for substantial orbital inclination (*2*). During pull-down capture, the absolute value of any vertical oscillation about the planetary orbital plane is largely preserved, but the planetocentric radius of the satellite orbit shrinks markedly. This means that the inclination of the satellite orbit about the planet is amplified during the pulldown. Figure 5 shows the evolution of a pair that is initially misaligned by only 0.6° in the circumstellar orbital plane. These initial cores both orbit the star in the prograde direction, but the mutual orbit is retrograde in the frame of the growing planet, so the initial inclination in the rotating frame is ~180°. The mass growth leads to rapid changes in orbital inclination as the orbit shrinks, eventually settling into a retrograde orbit but with substantial final inclination relative to the planetary orbital plane. This planet has the same mass growth as in Fig. 2.

Captured orbits also show a wide range of orbital eccentricities. The most eccentric of these get close enough to the planet that tidal dissipation in the satellite will likely circularize the orbit during the age of the star. However, we estimate, in the Supplementary Materials, that this is likely to occur only for those satellites whose orbits get within $\sim 16R_J$ of the planet. Given the estimated parameters of Kepler-1625b-i (semimajor axis in the range of 23 to 55 R_J), this suggests that the orbit of the satellite will still retain its original eccentricity. This is important, as it can affect the predictions for future transit events. It also implies that there may be a population of similarly massive satellites on more compact, circular orbits, awaiting discovery around giant planets.

The time scale of the planetary growth has an important effect on the outcome. Figure 6 shows the final semimajor axis and inclination for three different integrations of the pulldown of a $m_3 = 3 \times 10^{-5}$

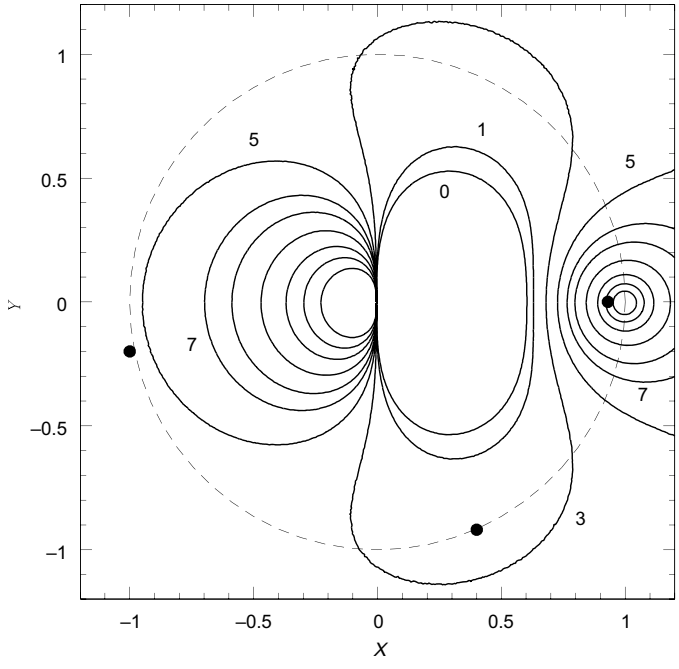

Fig. 3. Sensitivity of orbits to mass growth. The solid contours show the value of the derivative $\partial C/\partial m_2$ of the Jacobi constant with respect to mass. Contours are calculated by $\Delta C/\Delta m_2$ for the cases $m_2 = 1.4 \times 10^{-4}$ and 9×10^{-5} and are labeled from 0 to 7. Additional contours are shown for values of 9, 13, 20, 30, and 50. The dashed line shows a circle of radius unity in these units, and the three solid points show the initial starting positions of the three examples of orbital evolution shown in Fig. 4. The essential feature to note here is that C is most sensitive to changes in m_2 in the vicinity of m_2, and this is where the most marked changes in orbital properties occur.

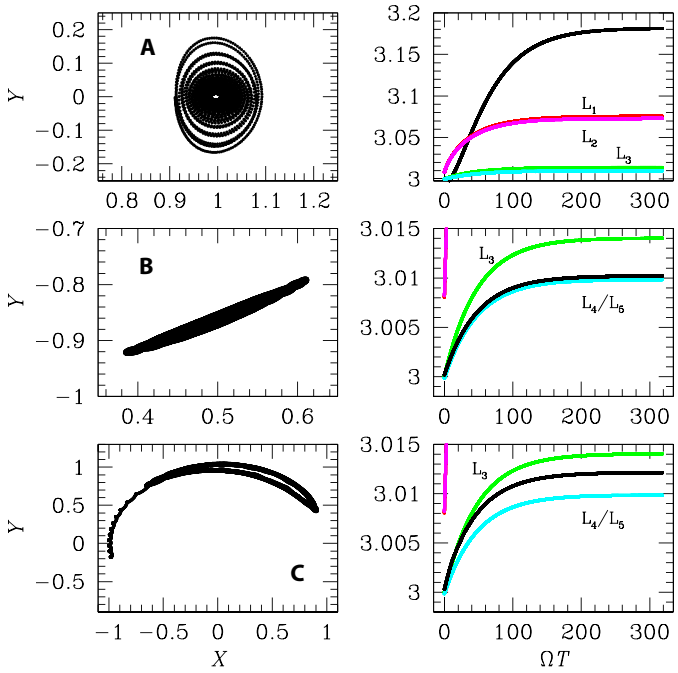

Fig. 4. Evolution of orbital families. (**A**) shows the orbital evolution of one of the Henon f-type orbits under the effect of mass growth. On the right, the black curve shows the evolution of the Jacobi constant *C* for this orbit as the mass grows. The critical values corresponding to the L_1, L_2, L_3, and L_4 points are shown in red, magenta, green, and cyan, respectively. The fact that the black curve crosses all of these curves is responsible for the change in orbital character, resulting in final orbit that is bound to m_2. (**B**), on the other hand, shows an orbit that starts near the L_5 point (thus, of the tadpole family). This orbit evolves far less under the same mass growth (which is the same for all three cases shown here) because the Jacobi constant is much less sensitive to the mass ratio in this location (see Fig. 3). The right-hand middle panel shows why: The black curve traces the evolution of the critical curve (in cyan) very closely, and so, the orbital structure does not change. (**C**) shows an intermediate case: an orbit that starts off as a horseshoe orbit but which evolves into a tadpole orbit about L_4 because the *C* of the orbit does not quite keep track with the critical value for L_3 and eventually dips slightly below it.

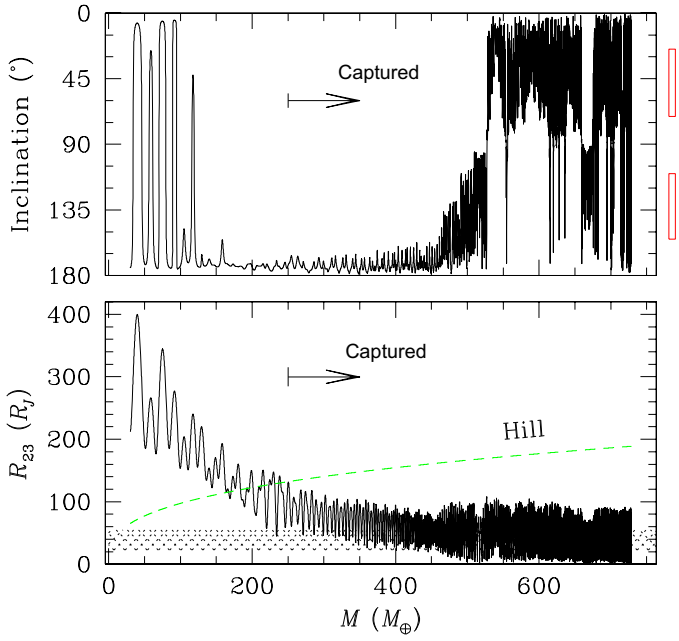

Fig. 5. Excitation of orbital inclination. (**Top**) Amplification of orbital inclination, relative to the planetary orbital plane, during pull-down capture. The red bars on the right indicate the estimated inclination for Kepler-1625b-i (the observations cannot tell the difference between prograde and retrograde orbits). (**Bottom**) The evolution of the separation due to mass growth, as in Fig. 2, but now from an initial orbit inclined by 0.6° from the star-planet orbital plane.

satellite. In each case, the initial value of the planet mass is $m_2 = 9 \times 10^{-5}$, and the final planet mass is 2.2×10^{-3}. The top shows a characteristic growth time scale $T_0 = 10$, comparable to the dynamical time of the gas at this location. The middle shows the case for $T_0 = 100$ (this is the case shown in Fig. 3), and the bottom shows the case for $T_0 = 1000$. In the first two cases, the integration is for $T = 500$, and in the third case, the integration is for $T = 5000$. As T_0 increases, the final states are more tightly bound and of lower inclination. The efficiency of capture also drops significantly with increasing T_0. The initial separations of the simulations in Fig. 6 are drawn uniformly from 2 to 10 initial Hill radii, and the velocities are drawn uniformly from the range that allows stable initial orbits. Inclinations are drawn uniformly from 0° to 2°. Integrating forward, in each case, 10^4 samples from these conditions yield a capture efficiency of 8.5% for $T_0 = 10$, which drops to 2.1% for $T_0 = 100$ and 0.3% for $T_0 = 1000$. The latter two values produce very few systems in the observed range of separation and inclination. If systems like Kepler-1625b-i turn out to be common, then they would argue in favor of a model in which the bulk of the mass of gas giant planets is accreted within a few local dynamical times.

DISCUSSION

The inferred radius and mass of the satellite Kepler-1625b-i (*2*) are consistent with the expected properties of a giant planet core before the dynamical instability stage of the core accretion scenario [e.g., (*15*)]. We suggest that multiple potential giant planet cores were growing on similar orbits in this system. Such a crowded location is a consequence of the proposal that planet growth is enhanced at particular locations in a protoplanetary disk, so-called "planet traps" (*18*), where hydrodynamical and/or chemical conditions conspire to enhance the growth rates of planetary cores and to slow their radial migration. Similar conditions may arise from the assembly of planetary cores in the presence of eccentricity dissipation (*19*). When the first planet to enter the dynamically unstable phase starts to grow, the changing gravitational interactions will perturb the remaining cores and can lead to a variety of outcomes. As discussed in Results, the dynamical evolution of coorbital bodies varies depending on their position relative to the accreting planet. The objects that show the most marked evolution are those that spend the most time in close proximity to the growing planet. It was shown that a stable class of these orbits exists in the context of the Hill problem (*20*) and in the more general context of bodies with finite masses (*21*). In the Supplementary Materials, we describe the properties of this orbital family in the mass range of interest (that of giant planet cores of mass ~10 to $30 M_\oplus$). During the mass growth, these nearby objects are dragged down closer to the planet, resulting in a final orbit well within the Hill sphere, i.e., a permanently captured satellite. Objects that exhibit tadpole or horseshoe orbits before the accretion remain stable and end up more tightly bound in these configurations (*22*). Other orbits can become destabilized in the process. It has been proposed that Uranus and Neptune may also be proto-giant planet cores that were originally formed in the

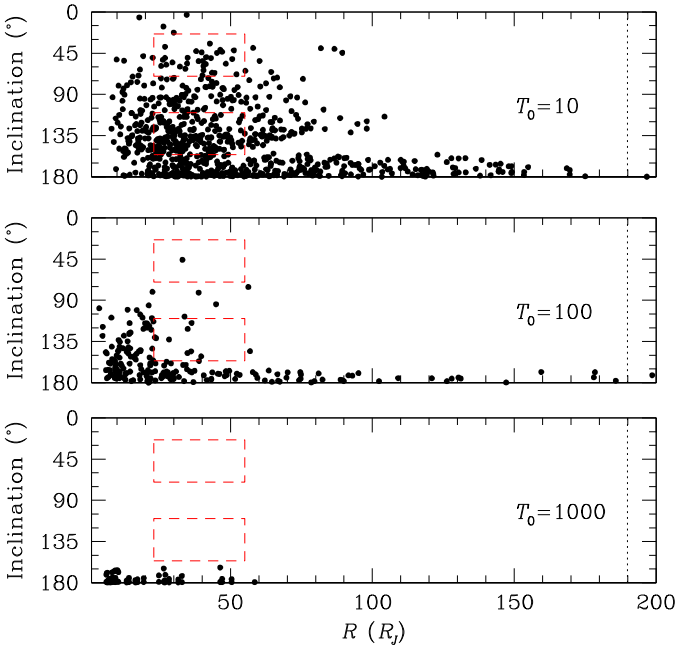

Fig. 6. The sensitivity to growth time scale. The speed at which the giant planet mass grows has an effect on the efficiency of the pull-down capture process. (**Top**) The result of 10^4 integrations of the pulldown of a mass $m_3 = 3 \times 10^{-5}$ during the growth of a planet from $m_2 = 3 \times 10^{-5}$ to $m_2 = 2.2 \times 10^{-3}$, with a characteristic growth time of $T_0 = 10$. The horizontal axis shows the final separation of the satellite from the planet, in units of Jupiter radii, and the vertical axis shows the maximum inclination achieved by the orbit during the last 100 time units (amounting to 12 planetary orbital periods). The boxes marked with red dashed lines correspond to the approximate range inferred from observations (*2*), and the vertical dotted line indicates the final Hill radius. The (**middle**) is calculated in the same way, except that $T_0 = 100$, and the (**bottom**) shows the same but for $T_0 = 10^3$. It is clear that the observations favor small T_0. In each panel, the maximum angle of deviation from coplanar orbits is shown, as discussed in Fig. 4.

Jupiter-Saturn region and scattered outward (*23*) as Jupiter and Saturn grew, and they may represent the outcome of this pathway.

The efficiency of the capture depends primarily on the speed with which the giant planet mass grows during the epoch at which the satellite crosses into the Hill sphere. Hence, stability depends only weakly on the final planet mass, although late-time mass growth will draw the satellite closer to the planet. A massive satellite may also restrict the inflow of gas to form more traditional satellites if these are formed from a disk that is supplied continuously (*5*) but may still allow formation of a traditional moon population in the case where the disk is a consequence of the initial collapse (*4*).

It is too early to tell whether such massive satellite configurations are rare or common, as the observed system is right at the edge of detectability and may represent the tip of an iceberg still to be recovered. However, there are hints that Neptune mass planets, comparable to Kepler-1625b-i, may be more numerous than expected from current models of giant planet formation. These claims have recently been made on the basis of microlensing surveys (*24*) and studies of transitting planets (*25*). Such an overabundance is consistent with our scenario in which many cores inhabit the giant planet formation region initially but only some are allowed to grow to giant planet masses. In such an event, we also anticipate that objects with mass similar to Kepler-1625b-i may also be captured into other stable configurations, such as Trojan orbits. This predicted population is also presently at the limit of detectability, but potential signatures of this type have been reported recently (*26*, *27*).

In this model, the parameters of Kepler-1625b-i also provide an important glimpse into the properties of a poorly understood phase of the core accretion model. Descriptions of the initial growth of giant planet envelopes assume hydrostatic equilibrium, an approximation that fails when the core reaches $\sim 100 M_\oplus$ (*15*). The final mass of the planet is determined by the properties of the gas disk and the rate at which mass can be supplied viscously to the planetary location (*16*). However, in between these two limits, the evolution of the planetary mass is a consequence of the dynamical instability of the disk gas in the vicinity of the growing core, a phase that is still poorly captured by current models although it is responsible for a substantial fraction of the mass growth of the planet. The efficiency of the pull-down process is a function of the speed of growth in this phase. If we repeat the calculation, from the same initial conditions but with a longer growth time, then the pull-down capture becomes increasingly inefficient for growth times >30 orbital times. As shown in the Supplementary Materials, this is a consequence of the fact that the phase space for stable orbits narrows when the planetocentric radius is of the order of the Hill sphere radius. If the mass growth is fast enough, then the satellite can be pulled down through the unstable region before orbital instabilities have a chance to grow. If the mass growth is too slow, then the orbit becomes unstable and the satellite undergoes a close encounter with the planet and is scattered out of the co-orbital region. The range of final inclinations is also larger for shorter growth times, as shown in Fig. 6. A larger sample of these orbits, with constraints on orbital eccentricity and inclination, could provide a probe of the growth time scale.

If Kepler-1625b-i were a rocky body, then it might provide an interesting alternative environment for studying planetary habitability, as the level of insolation that it receives from the host star is compatible with broad definitions of planetary habitable zones (*2*). If our interpretation is correct, then this body is more accurately described as a proto-giant planet core, isolated from the gas disk before it had a chance to exceed the threshold for runaway gas accretion. However, even in this stage, it should host a gaseous envelope of similar mass to its rocky inventory (*10*), which is consistent with the estimated radius and too thick to enable Earth-like conditions. On the other hand, studies of objects such as Kepler-1625b-i can provide an invaluable snapshot into a phase of giant planet evolution that is usually hidden beneath several hundred Earth masses of gas.

SUPPLEMENTARY MATERIALS

Supplementary material for this article is available at http://advances.sciencemag.org/cgi/content/full/5/10/eaaw8665/DC1

Supplementary Methods and Methods

Fig. S1. Retrograde stable orbits.

Fig. S2. Initial conditions for stable orbits.

References (*29*–*32*)

REFERENCES AND NOTES

1. S. J. Peale, Origin and evolution of the natural satellites. *Annu. Rev. Astron. Astrophys.* **37**, 533–602 (1999).
2. A. Teachey, D. M. Kipping, Evidence for a large exomoon orbiting Kepler-1625b. *Sci. Adv.* **4**, eaav1784 (2018).
3. R. Heller, K. Rodenbeck, G. Bruno, An alternative interpretation of the exomoon candidate signal in the combined Kepler and Hubble data of Kepler-1625. *Astron. Astrophys.* **624**, 95–102 (2019).
4. I. Mosqueira, P. R. Estrada, Formation of the regular satellites of giant planets in an extended gaseous nebula I: Subnebula model and accretion of satellites. *Icarus* **163**, 198–231 (2003).

5. R. M. Canup, W. R. Ward, Formation of the Galilean satellites: Conditions of accretion. *Astron. J.* **124**, 3404–3423 (2002).
6. R. M. Canup, W. R. Ward, A common mass scaling for satellite systems of gaseous planets. *Nature* **441**, 834–839 (2006).
7. M. Cilibrasi, J. Szulágyi, L. Mayer, J. Drążkowska, Y. Miguel, P. Inderbitzi, Satellites form fast & late: A population synthesis for the Galilean moons. *Mon. Not. R. Astron. Soc.* **480**, 4355–4368 (2018).
8. J. J. Fortney, M. S. Marley, J. W. Barnes, Planetary radii across five orders of magnitude in mass and stellar insolation: Application to transits. *Astrophys. J.* **659**, 1661–1672 (2007).
9. H. Ochiai, M. Nagasawa, S. Ida, Extrasolar binary planets. I. Formation by tidal capture during planet-planet scattering. *Astrophys. J.* **790**, 92–101 (2014).
10. A. S. Hamers, S. F. Portegies Zwart, Catching a planet: A tidal capture origin for the exomoon candidate *Kepler* 1625b I. *Astrophys. J. Lett.* **869**, L27–L32 (2018).
11. P. Goldreich, History of the lunar orbit. *Rev. Geophys.* **4**, 411–439 (1966).
12. B. M. S. Hansen, Calibration of equilibrium tide theory for extrasolar planet systems. *Astrophys. J.* **723**, 285–299 (2010).
13. V. Lainey, J.-E. Arlot, Ö. Karatekin, T. van Hoolst, Strong tidal dissipation in Io and Jupiter from astrometric observations. *Nature* **459**, 957–959 (2009).
14. T. A. Heppenheimer, C. Porco, New contributions to the problem of capture. *Icarus* **30**, 385–401 (1977).
15. J. B. Pollack, O. Hubickyj, P. Bodenheimer, J. J. Lissauer, M. Podolak, Y. Greenzweig, Formation of the giant planets by concurrent accretion of solids and gas. *Icarus* **124**, 62–85 (1996).
16. T. Tanigawa, M. Ikoma, A systematic study of the final masses of gas giant planets. *Astrophys. J.* **667**, 557–570 (2007).
17. E. Rabe, The Trojans as escaped satellites of Jupiter. *Astron. J.* **59**, 433–439 (1954).
18. F. S. Masset, A. Morbidelli, A. Crida, J. Ferreira, Disk surface density transitions as protoplanet traps. *Astrophys. J.* **642**, 478–487 (2006).
19. B. F. Collins, R. Sari, Co-orbital oligarchy. *Astron. J.* **137**, 3778–3787 (2009).
20. M. Hénon, Numerical exploration of the restricted problem. VI. Hill's case: Non-periodic orbits. *Astron. Astrophys.* **9**, 24–36 (1970).
21. J. D. Hadjidemetriou, D. Psychoyos, G. Voyatzis, The 1/1 resonance in extrasolar planetary systems. *Celest. Mech. Dyn. Astron.* **104**, 23–38 (2009).
22. H. J. Fleming, D. P. Hamilton, On the origin of the Trojan asteroids: Effects of Jupiter's mass accretion and radial migration. *Icarus* **148**, 479–493 (2000).
23. E. W. Thommes, M. J. Duncan, H. F. Levison, The formation of Uranus and Neptune in the Jupiter-Saturn region of the Solar System. *Nature* **402**, 635–638 (1999).
24. D. Suzuki, D. P. Bennett, S. Ida, C. Mordasini, A. Bhattacharya, I. A. Bond, M. Donachie, A. Fukui, Y. Hirao, N. Koshimoto, S. Miyazaki, M. Nagakane, C. Ranc, N. J. Rattenbury, T. Sumi, Y. Alibert, D. N. C. Lin, Microlensing results challenge the core accretion runaway growth scenario for gas giants. *Astrophys. J. Lett.* **869**, L34–L39 (2018).
25. D. Foreman-Mackey, T. D. Morton, D. W. Hogg, E. Agol, B. Schölkopf, The population of long-period transiting exoplanets. *Astron. J.* **152**, 206–223 (2016).
26. M. Hippke, D. A. Angerhausen, A statistical search for a population of exo-trojans in the *Kepler* data set. *Astrophys. J.* **811**, 1–5 (2015).
27. A. Leleu, J. Lillo-Box, M. Sestovic, P. Robutel, A. Correia, N. Hara, D. Angerhausen, S. Grimm, J. Schneider, Co-orbital exoplanets from close period candidates: The TOI-178 case. *Astron. Astrophys.* **624**, 46–54 (2019).
28. M. Gillon, A. H. M. J. Triaud, B.-O. Demory, E. Jehin, E. Agol, K. M. Deck, S. M. Lederer, J. de Wit, A. Burdanov, J. G. Ingalls, E. Bolmont, J. Leconte, S. N. Raymond, F. Selsis, M. Turbet, K. Barkaoui, A. Burgasser, M. R. Burleigh, S. J. Carey, A. Chaushev, C. M. Copperwheat, L. Delrez, C. S. Fernandes, D. L. Holdsworth, E. J. Kotze, V. Van Grootel, Y. Almleaky, Z. Benkhaldoun, P. Magain, D. Queloz, Seven temperate terrestrial planets around the nearby ultracool dwarf star TRAPPIST-1. *Nature* **542**, 456–460 (2017).
29. A. Socrates, B. Katz, S. Dong, Q in other Solar systems. arxiv:1209.5724 (2012).
30. D. Banfield, N. Murray, A dynamical history of the inner Neptunian satellites. *Icarus* **99**, 390–401 (1992).
31. K. Zhang, D. P. Hamilton, Orbital resonances in the inner neptunian system: II. Resonant history of Proteus, Larissa, Galatea & Despina. *Icarus* **193**, 267–282 (2008).
32. I. Adachi, C. Hayashi, K. Nakazawa, The gas drag effect on the elliptic motion of a solid body in the primordial solar nebula. *Prog. Theor. Phys.* **56**, 1756–1771 (1976).

Acknowledgments: Some of the simulations described here were performed on the UCLA Hoffman2 shared computing cluster and using the resources provided by the Bhaumik Institute. This research has made use of NASA's Astrophysics Data System. **Author contributions:** B.M.S.H. conceived of the idea, performed the calculations, and wrote the manuscript. **Competing interests:** The author declares that he has no competing interests. **Data and materials availability:** All data needed to evaluate the conclusions in the paper are present in the paper and/or the Supplementary Materials. Additional data related to this paper may be requested from the authors.

Submitted 31 January 2019
Accepted 9 September 2019
Published 2 October 2019
10.1126/sciadv.aaw8665

Citation: B. M. S. Hansen, Formation of exoplanetary satellites by pull-down capture. *Sci. Adv.* **5**, eaaw8665 (2019).